Structural basis for inhibition of the epidermal growth factor receptor by cetuximab

Shiqing Li,[1] Karl R. Schmitz,[1,2] Philip D. Jeffrey,[3,5] Jed J.W. Wiltzius,[4] Paul Kussie,[4] and Kathryn M. Ferguson[1,2,*]

[1]Department of Physiology, University of Pennsylvania School of Medicine, Philadelphia, Pennsylvania 19104
[2]Graduate Group in Biochemistry and Molecular Biophysics
[3]Memorial Sloan-Kettering Cancer Center, New York, New York 10021
[4]Protein Science Department, ImClone Systems, New York, New York 10014
[5]Present address: Department of Molecular Biology, Princeton University, Princeton, New Jersey 08544
*Correspondence: ferguso2@mail.med.upenn.edu

Summary

Recent structural studies of epidermal growth factor receptor (EGFR) family extracellular regions have identified an unexpected mechanism for ligand-induced receptor dimerization that has important implications for activation and inhibition of these receptors. Here we describe the 2.8 Å resolution X-ray crystal structure of the antigen binding (Fab) fragment from cetuximab (Erbitux), an inhibitory anti-EGFR antibody, in complex with the soluble extracellular region of EGFR (sEGFR). The sEGFR is in the characteristic "autoinhibited" or "tethered" inactive configuration. Cetuximab interacts exclusively with domain III of sEGFR, partially occluding the ligand binding region on this domain and sterically preventing the receptor from adopting the extended conformation required for dimerization. We suggest that both these effects contribute to potent inhibition of EGFR activation.

Introduction

Ligand-induced signaling from receptor tyrosine kinases (RTKs) of the epidermal growth factor receptor (EGFR) family (also known as ErbB or HER) regulates many cellular processes, including proliferation, cell motility, and differentiation (Holbro and Hynes, 2004). Perturbations in these cellular signals can lead to malignant transformation, and the correlation between EGFR and cancer has been firmly established (Arteaga, 2003; Mendelsohn and Baselga, 2003). Deregulation of EGFR can arise from its overexpression (Arteaga, 2002), mutation/truncation of the receptor (Boerner et al., 2003), or activation by aberrant autocrine growth factor loops (Normanno et al., 2001). EGFR has been implicated in the development of a wide range of epithelial cancers, including those of the breast, colon, head and neck, kidney, lung, pancreas, and prostate. In these settings, deregulation of EGFR correlates with decreased disease-free and overall survival (Gullick, 1991; Klijn et al., 1992; Sainsbury et al., 1985; Salomon et al., 1995). In the early 1980s, as details of the normal and oncogenic properties of EGFR were unfolding, it was proposed that EGFR signaling and cellular proliferation could be blocked by antibodies that interact with the extracellular region of EGFR, and prevent the binding of activating ligands: EGF, transforming growth factor α (TGFα), amphiregulin (AR), betacellulin (BTC), epigen (EPN), epiregulin (EPR), and heparin binding EGF-like growth factor (HB-EGF), collectively referred to as the EGF agonists (Mendelsohn, 2002). A panel of antibodies with such inhibitory properties was developed 20 years ago by immunizing mice with human A431 epidermoid carcinoma cells that express high levels of EGFR, selecting antibodies that bind specifically to the extracellular region of EGFR, and then screening for those that inhibit EGF binding and receptor phosphorylation (Gill et al., 1984; Kawamoto et al., 1983; Sato et al., 1983). The resulting antibodies inhibit cellular proliferation in vitro and in vivo (Masui et al., 1984; Mendelsohn, 1988). For one of these antibodies, mAb 225, a human:murine chimeric version was produced (Goldstein et al., 1995). This antibody, cetuximab (IMC-C225), marketed under the name Erbitux, has been the center of intensive study for its use as an anticancer agent (Graham et al., 2004) and was approved by the FDA in February 2004 for use in treating advanced-stage EGFR-expressing colorectal cancer.

Structural data published over the past few years have transformed our view of how EGFR is regulated by ligand binding,

SIGNIFICANCE

Members of the EGFR family are implicated in many human cancers and are the targets of several anticancer therapies. The anti-ErbB2 (HER2/Neu) antibody trastuzumab (Herceptin) is well established as a key element in treatment of metastatic ErbB2-positive breast cancers. In 2004, the anti-EGFR antibody cetuximab (Erbitux) was approved for treatment of advanced colorectal cancer. By contrast with trastuzumab, which does not prevent ligand-induced ErbB receptor activation, the primary mechanism of cetuximab is to block ligand-stimulated EGFR signaling. Our structure of sEGFR in complex with the antigen binding fragment of cetuximab reveals the molecular mechanism of its inhibition of ligand-induced EGFR dimerization and activation, and has important implications for the development of new strategies to target EGFR-positive cancers.

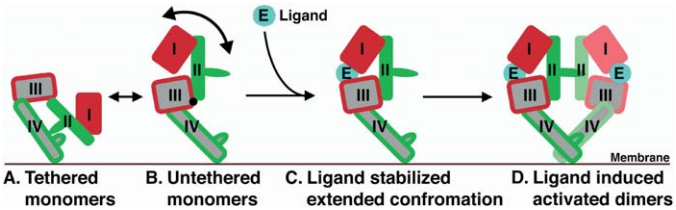

Figure 1. Mechanism of ligand-induced EGFR dimerization

The domains of the extracellular region of EGFR are shown in cartoon representation, with domain I in red, domain II in green, domain III in gray with red border, domain IV in gray with green border, and ligand in cyan. Most (about 95%) of the unliganded EGFR exists in a compact autoinhibited or tethered conformation, in which domains II and IV form an intramolecular interaction or tether (**A**). In the remaining 5% of the unliganded molecules, this tether is broken, and the sEGFR can adopt a range of untethered conformations (**B**), some of which will be more extended. Ligand binds preferentially to untethered molecules, and interacts simultaneously with domains I and III, stabilizing the particular extended form in which domain II is exposed and the receptor can dimerize (**C**). Dimerization is entirely receptor-mediated and dominated by domain II interactions (**D**) (J.P. Dawson, M.B. Berger, C.-C. Lin, J. Schlessinger, M.A. Lemmon, and K.M.F., submitted).

and have shed light on how agents that bind to the extracellular region of EGFR might inhibit EGFR activation (Figure 1) (Burgess et al., 2003). EGFR dimerization is entirely receptor-mediated, with no contacts between the two growth factor molecules in the dimeric complex (Garrett et al., 2002; Ogiso et al., 2002). By binding simultaneously to two sites (within domains I and III) in the extracellular region of the receptor, growth factor alters the spatial arrangement of the domains as shown schematically in Figure 1. This domain rearrangement exposes a critical region of domain II that is buried by an intramolecular interaction (or tether) with domain IV in the inactive receptor (Figure 1A). The region thus exposed is known as the dimerization arm, and forms the core of the dimer interface in Figure 1D. Growth factors bind preferentially to the extended or untethered forms of EGFR (Figure 1B) and "trap" the receptor in the conformation that can dimerize through the exposed dimerization arm (Figure 1C), thus driving the equilibrium shown in Figure 1 to the right.

Based on this mechanism, there are several possible ways that an inhibitor could bind to the extracellular region of EGFR and prevent receptor activation. Such an agent could act as an antagonist, and compete directly for ligand binding by interacting with the growth factor binding sites on the receptor. Alternatively, the agent could block ligand binding indirectly by stabilizing a receptor conformation that cannot bind growth factor with high affinity. In addition, receptor dimerization and activation could be blocked by occluding the domain II dimerization interface. The monoclonal antibody pertuzimab (2C4/Omnitarg) functions in this way, binding to domain II of ErbB2 (HER2/neu) and preventing its neuregulin-induced heterodimerization with ErbB3 (Agus et al., 2002; Franklin et al., 2004).

Here we describe structural studies that reveal the molecular mechanism of direct EGFR inhibition by the antibody drug cetuximab/Erbitux. A 2.8 Å resolution crystal structure of the cetuximab Fab fragment bound to the EGFR extracellular region shows that the antibody binds to a site on domain III of the receptor that overlaps the EGF binding site. In addition, cetuximab binding sterically prevents the EGFR extracellular region from adopting the dimerization-competent extended configuration depicted in Figures 1B–1D. These findings provide a structural framework for improving agents that inhibit EGFR by targeting its extracellular region.

Results and discussion

Binding of cetuximab to the soluble extracellular region of EGFR

The entire extracellular region of EGFR (sEGFR), corresponding to amino acids 1–618 of the mature protein with a C-terminal hexa-histidine tag, was produced by secretion from baculovirus-infected Sf9 cells exactly as described previously (Ferguson et al., 2000; Ferguson et al., 2003). The antigen binding (Fab) fragment of cetuximab (FabC225) was prepared by papain digestion of the IgG protein. Using Surface Plasmon Resonance (SPR/Biacore), we found that sEGFR binds to immobilized FabC225 (Figure 2A; black triangles) with a K_D value of 2.3 ± 0.5 nM, similar to that observed for binding of the Fab fragment of mouse mAb 225 to the EGFR in A431 cell homogenates (Fan et al., 1993). Cetuximab also efficiently inhibits binding of sEGFR to immobilized EGF (Figure 2C). Addition of equimolar FabC225 to a 600 nM sample of sEGFR abolishes the binding of sEGFR to immobilized EGF.

Structure determination

Crystals of the isolated Fab fragment of cetuximab that diffract to 2.0 Å resolution were grown from 1.8 M ammonium sulfate, 100 mM sodium citrate at pH 6.25. The structure was solved using molecular replacement (MR) methods with separate search models for the variable (Fv) and the constant (Fc) domains that were selected on the basis of sequence identity. The final, refined model contained two FabC225 molecules in the asymmetric unit. FabC225:sEGFR complex for crystallization was prepared by mixing a 2-fold molar excess of purified FabC225 with sEGFR, and separating the complex from excess Fab by size exclusion chromatography (SEC). Crystals of the FabC225:sEGFR complex that diffract to 2.8 Å resolution were grown from 15% PEG 3350, 250 mM $(NH_4)_2SO_4$, 100 mM imidazole, 10 mM $CdCl_2$ (pH 7.5). The structure was solved using MR methods with search models based on coordinates of sEGFR (PDB id 1NQL) and FabC225. The final model, refined to 2.8 Å resolution, contains amino acids 2–614 of sEGFR, amino acids 1–211 of the Fab light chain, amino acids 1–220 of the Fab heavy chain, a total of 19 carbohydrate residues, and 71 ordered water molecules. Crystallographic and refinement statistics are given in Table 1.

Conformation of sEGFR bound to cetuximab

Previously determined structures of dimeric and monomeric sEGFR (Burgess et al., 2003) have shown that the individual domains in the extracellular region are altered little (if at all) upon binding of activating growth factor. Rather, the intramolecular domain arrangement plays a primary role in the mechanism of receptor activation. As expected, the structure of each individual domain within FabC225-bound sEGFR is very similar to that seen in monomeric sEGFR and in the sEGFR/ligand complexes. The β helix or solenoid folds adopted by domains I and III are rigid structures, and are not altered significantly

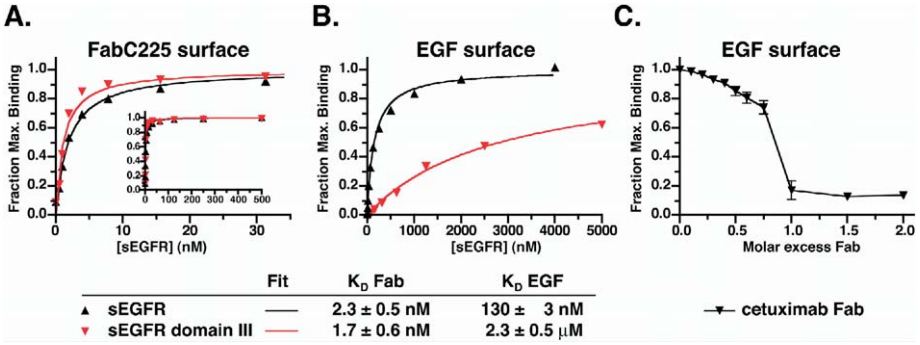

Figure 2. The cetuximab Fab fragment binds to sEGFR and inhibits sEGFR binding to EGF

A: Surface Plasmon Resonance (SPR) analysis of sEGFR binding to immobilized FabC225. A series of sEGFR samples of the indicated concentrations or of the domain III fragment of sEGFR (sEGFR-III) were passed over a Biosensor surface to which FabC225 had been covalently coupled. A representative data set of the equilibrium SPR response for each sample, expressed as the fraction of the maximum binding, is plotted as a function of the concentration of sEGFR. The inset shows that no additional binding is seen at higher concentrations. These data can be fit to a simple one-site Langmuir binding equation. The curve indicates the fit to the particular data set shown. K_D values are the mean of at least three independent binding experiments. K_D values are 2.3 ± 0.5 and 1.7 ± 0.6 nM for sEGFR and sEGFR-III, respectively.

B: SPR equilibrium binding analysis, as described in **A**, of a similar set of samples of sEGFR and sEGFR-III to immobilized EGF. K_D values are 130 ± 3 nM and 2.3 ± 0.5 μM for sEGFR and sEGFR-III, respectively.

C: The ability of FabC225 to compete with immobilized EGF for sEGFR binding is shown. The indicated molar excesses of Fab were added to samples of a fixed concentration of sEGFR (600 nM). The equilibrium SPR responses obtained by passing these mixtures over immobilized EGF, expressed as a fraction of the response with no added Fab, are plotted as a function of the molar excess of Fab. Each data point is the mean of at least three independent measurements. All binding is abolished at a 1:1 stochiometry of FabC225:sEGFR, and the IC_{50} value for these conditions is 500 nM.

upon binding of growth factor or FabC225. Comparing the structures of monomeric sEGFR with and without bound Fab, the root mean square deviation (rmsd) for Cα positions is 0.93 and 0.54 Å for domains I and III, respectively. Similarly, domain IV does not change significantly between these two structures (rmsd of 1.0 Å for Cα positions), nor does the relative orientation of domains III and IV. As discussed in more detail later, the conformation of domain II does differ between the two sEGFR structures—probably as a result of crystal packing.

The domain arrangement seen in sEGFR bound to FabC225 is similar to that previously observed for monomeric sEGFR (Ferguson et al., 2003) and for sErbB3 (Cho and Leahy, 2002) (Figure 3A). This conformation is characterized by an intramolecular interaction between domains II and IV that "tethers" the molecule in an autoinhibited conformation that is distinct from the extended conformation observed in the dimeric complexes of sEGFR with EGF (Ogiso et al., 2002) and with TGFα (Garrett et al., 2002). In the tethered conformation, the ligand binding sites on domains I and III are too distant from one other to both contact the same ligand molecule, and the dimerization

Table 1. Data collection and refinement statistics

	FabC225	FabC225:sEGFR complex
Data collection statistics[a]		
Space group	$P2_12_12_1$	$P2_1$
Unique cell dimensions	a = 64.4 Å, b = 82.0 Å, c = 211.4 Å	a = 77.8 Å, b = 70.9 Å, c = 147.1 Å; β = 102.5°
X-ray source	NSLS X9A	CHESS A1
Resolution limit	2.0 Å	2.8 Å
Observed/unique	635,708/73,414	143,424/38,621
Completeness (%)	95.6 (96.8)	98.9 (90.6)
R_{sym}[b]	0.07 (0.30)	0.05 (0.33)
<I/σ>	12.7 (5.5)	16.5 (5.6)
Refinement statistics		
Resolution limits	15–2.0 Å	50–2.8 Å
No. of reflections/no. test set	70,346/3,588	36,547/1,931
R factor (R_{free})[c]	0.22 (0.27)	0.22 (0.27)
Model		
Protein	2 FabC225 molecules	1 FabC225:sEGFR complex
		aa 2–614 (sEGFR); 18 saccharide units
	aa 1–213 (light chain)	aa 1–211 (light chain)
	aa 1–221 (heavy chain)	aa 1–220 (heavy chain); 1 saccharide unit
	353 water molecules	71 water molecules
Total number of atoms	7013	8152
RMSD bond lengths (Å)	0.012	0.013
RMSD bond angles (°)	1.76	1.66

[a] Numbers in parentheses refer to last resolution shell.

[b] $R_{sym} = \Sigma|I_h - \langle I_h \rangle| / \Sigma I_h$, where $\langle I_h \rangle$ = average intensity over symmetry equivalent measurements.

[c] R factor = $\Sigma||F_o| - |F_c|| / \Sigma|F_o|$, where summation is over data used in the refinement; R_{free} includes only 5% of the data excluded from the refinement.

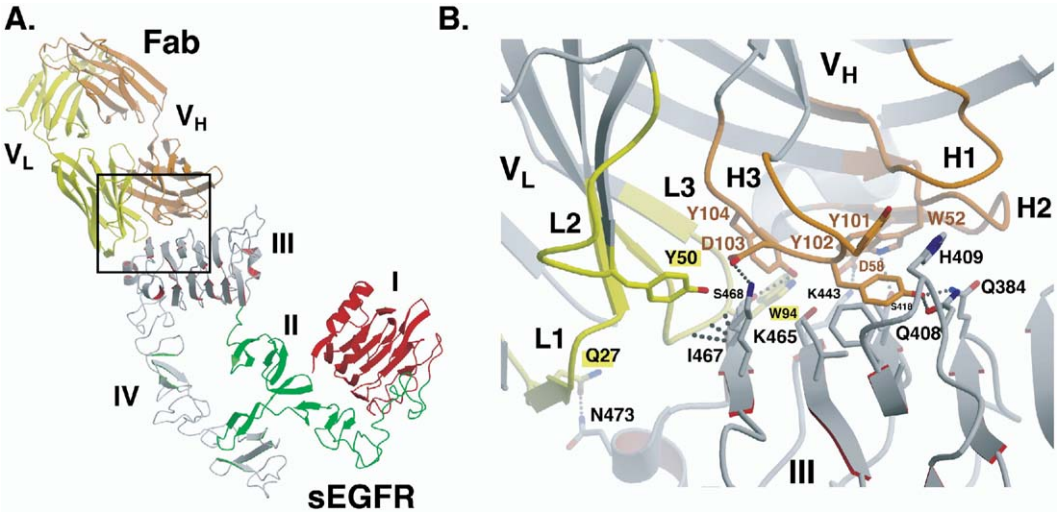

Figure 3. Cetuximab binds to domain III of a tethered sEGFR molecule

A: Ribbons representation of FabC225:sEGFR complex. The V_L chain of FabC225 is shown in yellow, the V_H chain in orange, domain I of sEGFR in red, and domain II in green. Domains III and IV are in gray, with the edges of the secondary structure elements in red and green, respectively. The box indicates the area of detail shown in **B**.

B: Closeup view of the FabC225:sEGFR interface. The CDRs are colored yellow for the V_L chain and orange for the V_H chain, and the remainder of the FabC225 is colored gray. Side chains that make key interactions are shown. Amino acid labels are colored orange for the V_H of FabC225, black on a yellow background for FabC225 V_L, and black on a white background for sEGFR. Hydrogen bonds are indicated with a dashed gray line.

interface on domain II is occluded by the intramolecular tether interaction.

The previously described structure of tethered sEGFR was obtained using crystals that were grown at pH 5.0, and that contained an EGF molecule bound weakly to the domain I ligand binding site (Ferguson et al., 2003). The structure described here represents the first structure of sEGFR with no bound growth factor ligand and at neutral pH. The common tethered configuration observed in these two sEGFR structures supports our previous conclusion that this tethered sEGFR configuration is the predominant unliganded form of the receptor (Ferguson et al., 2003). Further, since cetuximab is an inhibitor of EGFR, this also strengthens our conclusion that the tethered form represents an inactive state of the EGFR extracellular region. Minor differences in the arrangement of the domains in the two tethered structures of sEGFR are discussed below.

The cetuximab binding site on sEGFR

The cetuximab Fab fragment binds exclusively to domain III, covering an epitope that partially overlaps the growth factor binding site on that domain (see below). Both the heavy and the light chains of cetuximab participate in the interaction with domain III, with all contacts coming from the complementarity determining regions (CDRs) of FabC225 (Figure 3B). CDRs L3 and H3 contribute the majority of the interactions with the receptor, and there are additional contributions from CDRs L1 and H2. Such a distribution of interactions is common in antibody-antigen complexes (Sundberg and Mariuzza, 2002). The binding surface of FabC225 is rich in tyrosines and tryptophans, as is also typical for antibody combining sites (Lo Conte et al., 1999). A total of 882 Å^2 of solvent accessible surface area on domain III is buried by FabC225 (a similar area is occluded from solvent on the Fab so that the total solvent accessible surface buried on formation of the FabC225:sEGFR complex is 1770 Å^2). Approximately two-thirds of the buried surface area on domain III is occluded from solvent by the heavy chain of FabC225. The overall shape complementarity (sc) parameter for the FabC225:sEGFR interface is 0.71 (Lawrence and Colman, 1993). This is larger than typically observed for an antibody-antigen binding interface (Lawrence and Colman, 1993), but is similar to that observed for the interaction of sErbB2 with both trastuzumab (Cho et al., 2003) and pertuzumab (Franklin et al., 2004). A higher sc parameter correlates with a higher-affinity antibody-antigen interaction (Li et al., 2003) and is thus expected for antibody drugs that have been selected, in part, for tight binding to their target.

The conformation of FabC225 is not altered significantly upon sEGFR binding. The backbone conformations of bound and unbound FabC225 are very similar (rmsd for Cα positions of V_L is 0.45 Å, and for V_H is 1.1 Å), and there is only a small (15°) decrease in the elbow angle in the bound structure. Notably, the conformations of the CDRs of FabC225 are essentially identical with and without bound sEGFR.

The light chain of FabC225 interacts with the C-terminal region of domain III. Q27 at the tip of CDR L1 makes the only side chain to side chain hydrogen bond between V_L and the receptor, interacting with N473 at the beginning of the C-terminal helix of domain III (Figure 3B). An extensive network of intermolecular main chain hydrogen bonds between CDR L3 and the most C-terminal strand of the domain III β helix contributes most of the light chain interactions, and serves to position the side chain of W94 of CDR L3 to interact with the aliphatic portion of K443 on the adjacent strand from the domain III β helix. CDR L2 contributes little to the interaction, although the side chain of Y50 makes a small contribution to the hydrophobic pocket that surrounds I467 from the receptor.

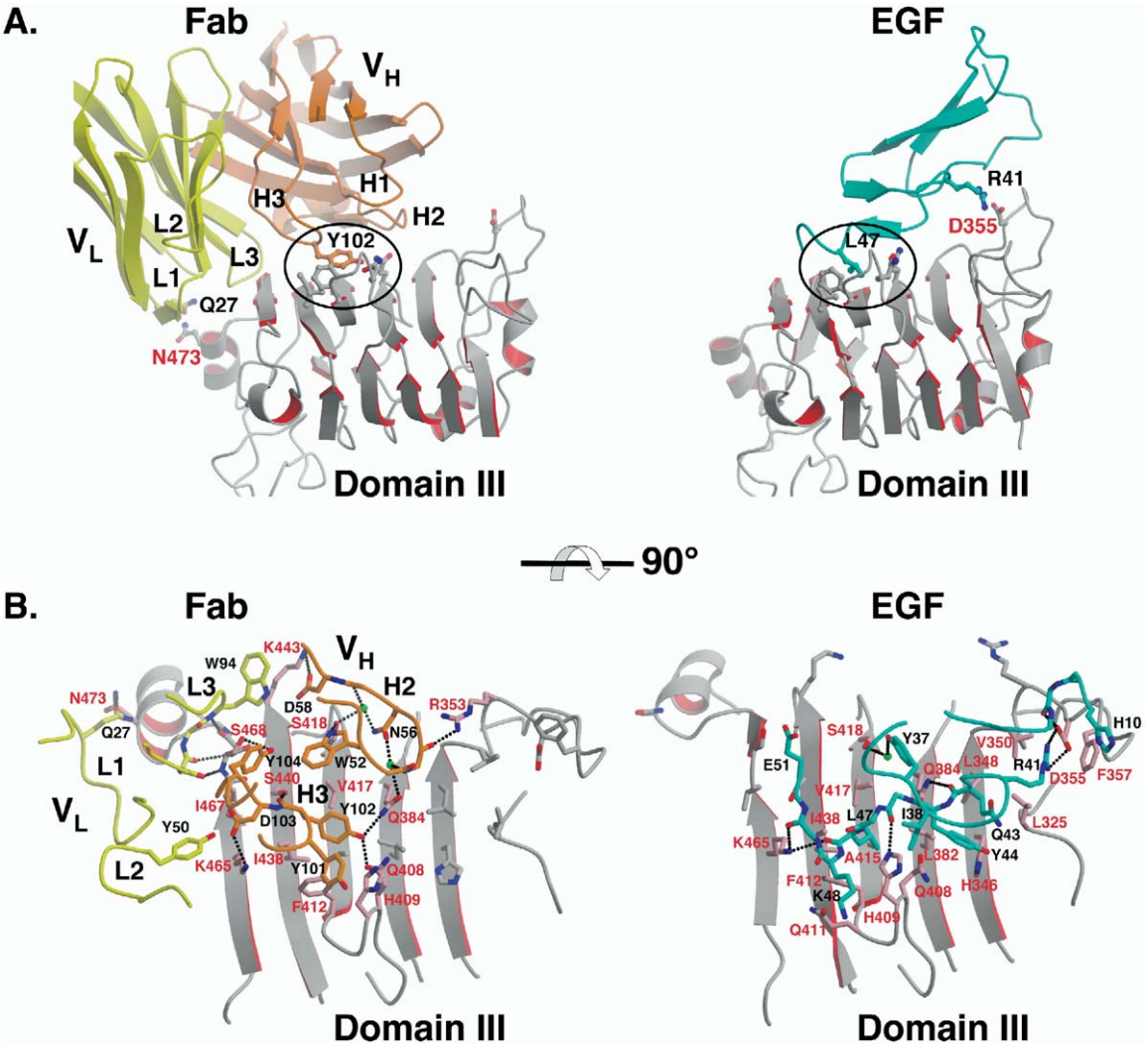

Figure 4. The cetuximab epitope partially overlaps the ligand binding region on domain III

A: The binding site region of the FabC225:sEGFR complex with domains colored as in Figure 2. The central Y102 from CDR H3 is shown, as are the side chains on sEGFR that contribute to the hydrophobic binding (ringed in black). Q27 from CDR L1 and N473 from sEGFR that form a direct hydrogen bond are also shown. The sEGFR:EGF complex is shown with domain III in the same orientation. Domains I and II of sEGFR are not drawn so that the ligand binding region can be seen. L47 of EGF occupies the same binding pocket as Y102 of FabC225 (ringed in black). R41 from EGF and D355 from sEGFR that make a critical salt bridge are also shown.

B: Detailed view of the interactions of domain III of sEGFR with FabC225 and with EGF. The view is looking down onto the binding site (90° rotation about the indicated axis). Only those parts of FabC225 and EGF that are directly involved in binding to this domain are shown. Side chains from FabC225 and EGF that interact with sEGFR are labeled in black. The same set of side chains on the sEGFR are shown in both panels. Where these residues are involved in interaction, they are colored pink and marked with red labels. Hydrogen bonds are shown with dotted black lines. Key water molecules are shown as green spheres.

The majority of the specific interactions between FabC225 and sEGFR come from the CDRs H2 and H3. At the center of the interface is a tyrosine from CDR H3 (Y102) that protrudes into a hydrophobic pocket on the surface of the large β sheet of domain III (see Figures 3B and 4), its hydroxyl group ideally placed to make hydrogen bonds with two glutamine side chains from sEGFR (Q384 and Q408). CDRs H2 and H3 of FabC225 are anchored over this hydrophobic pocket on domain III by a series of interactions that include two salt bridges (D58[V_H] to K443[sEGFR] and D103[V_H] to K465[sEGFR]), two further side chain to side chain hydrogen bonds (W52[V_H] to S418[sEGFR] and Y104[V_H] to S468[sEGFR]), two side chain-to-main chain hydrogen bonds (between the G54 and D103 carbonyl oxygens from V_H and the S440 and R353 side chains from sEGFR), plus indirect hydrogen bonds linking N56(V_H) with S418 and Q384 from EGFR through two highly ordered water molecules (Figures 3B and 4B). Such water-mediated hydrogen bonds are common in antibody-antigen interactions (Sundberg and Mariuzza, 2002), and there are likely more ordered waters in this interface that cannot be modeled with any confidence at the resolution of this structure.

As described above, all of the interactions between the ce-

tuximab Fab and sEGFR are with domain III of the receptor, with no interactions to domain I, or indeed domains II or IV. To confirm that only domain III is required for the high-affinity interaction of FabC225 with sEGFR, we generated recombinant baculovirus to direct expression and secretion from Sf9 cells of isolated domain III (amino acids 310–514 of mature EGFR). As shown in Figure 2A (red points and curve) the affinity of isolated domain III for immobilized FabC225 is the same as that observed with full-length sEGFR. By contrast, the binding of isolated domain III to EGF is substantially weaker than for full-length sEGFR (Figure 2B), as previously reported for a proteolytically derived sEGFR fragment that encompasses domain III (amino acids 302–503) (Kohda et al., 1993; Lemmon et al., 1997). Whereas high affinity binding of growth factor ligand requires both domains I and III of sEGFR, cetuximab Fab efficiently blocks growth factor binding through high-affinity interaction with domain III alone.

Table 2. Comparison of interaction of domain III of sEGFR with FabC225, EGF, and TGFα

	FabC225: sEGFR	sEGFR: EGF[a]	sEGFR: TGFα[a]
Number of hydrogen bonds (≤3.5 Å)[b]	10	5	5
Salt bridge interactions	2	1	1
Area of domain III buried by ligand (Å²)[c]	882	810	729
Polar area	440	299	248
Apolar area	442	511	481
Shape complementarity	0.71	0.70	0.70

[a] Values are for the interaction between chains A (sEGFR) and C (EGF/TGFα). Values are similar for the other complex.
[b] Defined using the program HBPLUS (McDonald and Thornton, 1994).
[c] The total surface area buried in the complex is approximately twice this value since an almost equal area of surface on the FabC225 also becomes solvent-inaccessible in the complex.

Comparison of sEGFR binding sites for cetuximab and EGF/TGFα

Figure 4 compares the interfaces formed by domain III with FabC225 and EGF, respectively, and illustrates how the binding site for the cetuximab Fab partially overlaps the domain III EGF binding site (Garrett et al., 2002; Ogiso et al., 2002). Y102 on CDR H3 of FabC225 occupies approximately the same position on the surface of sEGFR (ringed in Figure 4A) as does an essential leucine side chain from the growth factor (L47 in EGF, L48 in TGFα). Both EGF and TGFα pack more deeply into the binding pocket in this region of sEGFR than FabC225. The packing for FabC225 is augmented by two side chain hydrogen bonds between the Y102 hydroxyl and glutamines on sEGFR (Q384 and Q408). By contrast, there are no side chain to side chain hydrogen bonds in this region when growth factors bind sEGFR. The only side chain to side chain interaction that occurs with domain III in the growth factor complexes is a salt bridge between an arginine on the ligand (R41 in EGF and R42 in TGFα) and an aspartate (D355) near the N-terminal part of the domain III β helix. There are no contacts between FabC225 and this region of domain III. Rather, as described above, FabC225 makes additional contacts with the C-terminal end of domain III that are not part of the EGF binding site, as shown in Figure 4.

The affinity of the FabC225:sEGFR interaction is 3 orders of magnitude higher than that for interaction of EGF with isolated domain III, and 50-fold greater than for the interaction between EGF and full-length sEGFR (where domain I also contributes). It is not immediately clear from the crystal structures what is the origin of the approximately 4.5 kcal/mol additional binding energy for FabC225 binding to domain III of sEGFR relative to the interaction of the growth factor ligands. A larger buried surface area is often associated with a stronger interaction (Lo Conte et al., 1999), and the surface area of domain III that is buried by FabC225 is larger than that buried by the growth factors (882 Å² for FabC225 versus 810 Å² and 729 Å² for EGF and TGFα, respectively; see Table 2). However, the additional buried surface area is largely polar, and the total apolar buried surface area on domain III in the FabC225:sEGFR complex is actually less than that for EGF or TGFα binding. Thus, the larger buried surface area does not provide a simple explanation for the increase in binding energy. This contrasts with a recent study that compared a series of antibodies with differing affinities for the same epitope on hen egg white lysozyme (Li et al., 2003). In this study, higher affinity of the antibody for the antigen tracked with an increase in the proportion of apolar buried surface area. The interface between the growth factor ligands and domain III is more apolar (≈65%) than typically observed in this type of protein-protein interaction, yet is of rather low affinity. The proportion of polar surface (≈50%) buried in the FabC225:sEGFR is typical for a high-affinity antigen-antibody interaction (Li et al., 2003; Lo Conte et al., 1999). The shape complementarity (sc) parameter for the interaction of FabC225 with sEGFR is quite high for an antibody-antigen interaction, and is similar to that for the interaction of EGF and TGFα with domain III of sEGFR.

As would be expected in a more polar interface, there are a greater number of hydrogen bonds between FabC225 and domain III of sEGFR than observed for the growth factor complexes (Table 2). There is no simple correlation between the number of hydrogen bonds or salt bridges in a protein-protein interaction and the observed affinity of a complex. Due to the large energy associated with desolvation of charged and polar groups at the interface upon formation of a protein-protein complex, these interactions are typically considered unfavorable (Honig and Nicholls, 1995) and are more usually considered to define specificity. In some cases, however, polar and charged interactions can contribute significantly to the binding energy (Sheinerman et al., 2000). Two features that have been pointed out as indicators of stabilizing charged and polar interactions (Sheinerman and Honig, 2002) are observed in the interaction of FabC225 and sEGFR. As can be seen in Figure 4B, the hydrogen bonds in the interface form a network that is likely even more extensive with the participation of ordered water molecules that cannot be modeled with accuracy at the resolution of this structure. Such networks stabilize charged and polar interactions. The second issue relates to the structure of free antibody. Two aspartates (D58 and D103) that participate in salt bridges in the FabC225:sEGFR complex are partially buried in the free antibody structure, which will reduce the energy required to desolvate these charged groups, resulting in a potentially higher contribution of these salt bridges to the strength of the interaction.

As discussed above, neither the structure of the antibody nor the structure of domain III changes upon binding. By contrast, the growth factor ligands appear to be quite flexible. In

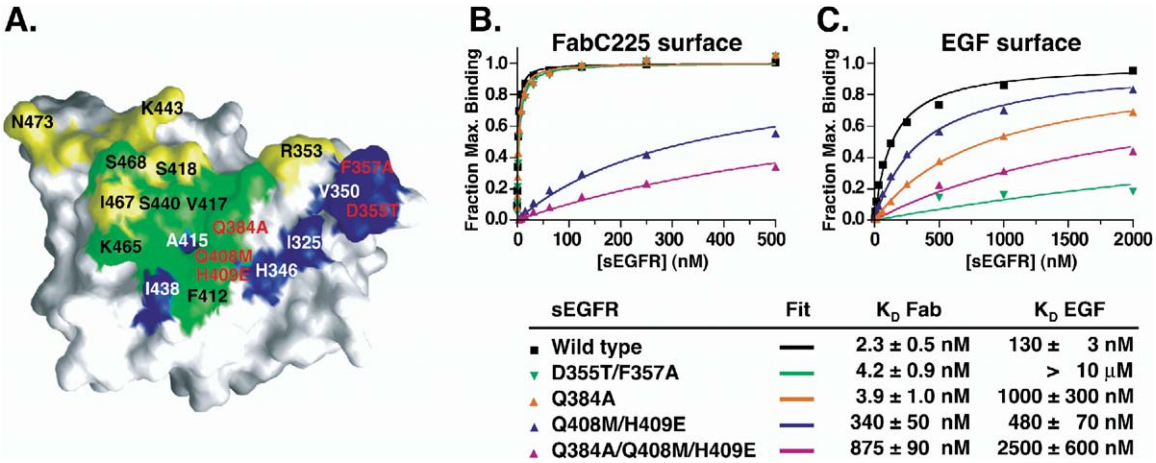

Figure 5. Mutational analysis of cetuximab epitope on sEGFR

A: A solvent-accessible surface representation of domain III in the same orientation as in Figure 4B. The surface is colored according to whether it interacts with EGF only (blue), FabC225 only (yellow), or both (green). The positions of the side chains shown in Figure 4B are indicated. The amino acids altered for the binding studies in **B** are shown in red.

B: Binding of altered sEGFR to immobilized FabC225. Data are presented as described in Figure 2A. In each case, the SPR response is expressed as a fraction of the maximum response for wild-type sEGFR.

C: Binding of the same sEGFR samples to immobilized EGF.

the crystal structure of isolated EGF there are two molecules in the asymmetric unit that each adopt a different conformation (Lu et al., 2001). Similarly, NMR structures of EGF (Cooke et al., 1987; Montelione et al., 1987) and TGFα (Kline et al., 1990; Tappin et al., 1989) suggest that regions involved in interaction with sEGFR are quite disordered. A disorder to order transition in the ligand upon binding to sEGFR may be one origin of their weaker affinity for sEGFR relative to binding of the antibody, rather than any difference in the nature of the interactions with domain III. It should be noted that this consideration may suggest that useful (flexible) antagonistic ligand analogs are unlikely to emerge.

Mutations in domain III differentially affect the binding of sEGFR to EGF and to cetuximab Fab

To confirm that the C225 epitope observed in the crystal accurately reflects that seen in solution, we generated mutations in two regions on the face of the large β sheet of domain III (Figure 5), in an effort to selectively impair EGF binding, antibody binding, or both. Substitution of the aspartic acid at position 355 with threonine, and of the phenylalanine at position 357 with alanine, has no effect on binding of sEGFR to immobilized FabC225 (as expected, since these amino acids are not part of the cetuximab epitope). However, as expected, since these side chains are involved in binding to growth factor ligand, this sEGFR variant binds immobilized EGF more than 100-fold more weakly than wild-type sEGFR (Figures 5B and 5C). By contrast, mutations in the region near the hydrophobic pocket that accommodates the leucine side chains of the growth factor ligand and the tyrosine 102 of the FabC225 disrupt binding of sEGFR to both FabC225 and EGF. A double mutant Q408M/H409E shows a 150-fold reduction in FabC225 binding, but only a 3.5-fold decrease in EGF binding. Additional alteration of Q384A results in a ≈1 μM K_D in both cases (Figure 5).

Comparison of domain II conformation in sEGFR structures

As mentioned above, the structures of domains I and III do not change upon binding of growth factor or antibody, and domain IV is unaffected by FabC225 binding. However, alterations in domain II are detected when the different sEGFR structures are compared, and these warrant some comment. Differences in domain II conformation result in a change in the relative orientations of domains I and III when the tethered sEGFR structure reported here is compared with the previously published pH 5 structure (Ferguson et al., 2003). With respect to domain III, the position of domain I in the two structures differs by a 50° rotation around an axis that is approximately parallel to the long axis of the domain II dimerization arm. This difference is not caused by the EGF that is weakly bound to domain I in the pH 5.0 tethered structure: an EGF molecule can easily be accommodated at the domain I binding site in the FabC225:sEGFR structure. Rather, we suggest that these structures provide two snapshots of a flexible domain II, which have been trapped by different crystal packing environments. An overlay of domain II from each crystal structure of sEGFR and of sErbB3 is shown in Supplemental Figure S1. The differences in the conformation of domain II in the two tethered structures lie almost entirely in the N-terminal half of this domain. By contrast, the conformation of the C-terminal half of domain II is similar for each tethered structure but distinct from the conformation of this region of domain II in the dimeric structures.

Influence of cetuximab on the conformation of sEGFR

Although cetuximab does not affect the structure of the individual domains in sEGFR, its binding to the tethered state of sEGFR will influence the distribution of conformations that are accessible to sEGFR. For unliganded sEGFR, some 5% of the receptors are estimated to be untethered and to adopt a range of extended conformations (Burgess et al., 2003; Ferguson et

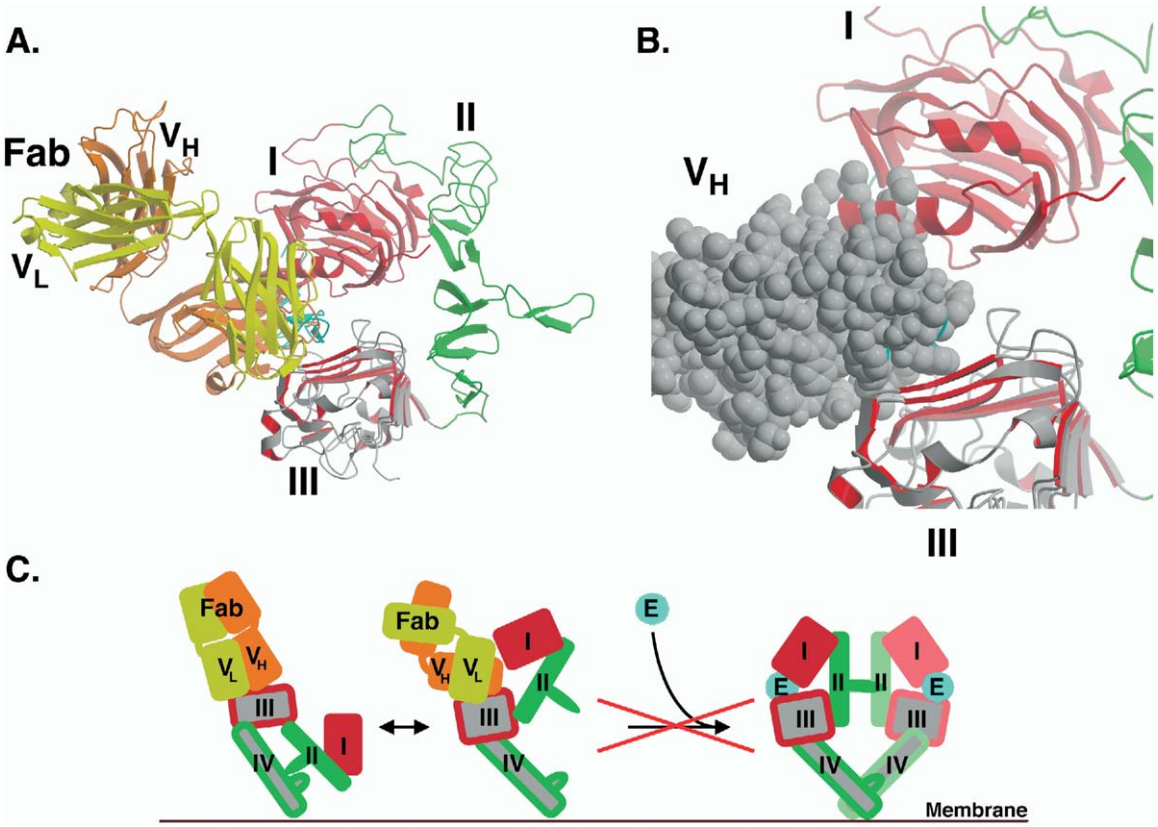

Figure 6. Cetuximab prevents sEGFR from adopting the extended conformation

A: One molecule from the sEGFR:EGF dimer is shown, with domains colored as in Figure 3 and EGF in cyan. Domain III from the FabC225:sEGFR complex was superimposed on domain III from this sEGFR:EGF complex. Only the FabC225 from the FabC225:sEGFR complex is shown, with colors as in Figure 3. A portion from the V_H domain of FabC225 (orange) clashes with EGF and with domain I from the sEGFR:EGF complex.

B: The V_H region of FabC225 is shown in space-filling representation to highlight the steric clash that would occur between this part of FabC225 and the N-terminal portion of domain I.

C: Model for inhibition of ligand-induced dimerization by cetuximab. In addition to blocking the domain III ligand binding site, FabC225 prevents the receptor from adopting the extended conformation required for high-affinity ligand binding and dimerization.

al., 2003). Cetuximab binding to domain III restricts the range of extended conformations available to this untethered population of receptors. Most importantly, the extended conformation that is required for dimerization is inaccessible to FabC225-bound sEGFR. By superimposing domain III from the FabC225:sEGFR complex with domain III from the sEGFR:EGF complex (Ogiso et al., 2002), it is apparent that FabC225 not only overlaps with the bound EGF but also with parts of domain I (Figure 6). With cetuximab bound to EGFR, the V_H region of the antibody sterically blocks domain I from occupying the position observed in the ligand-bound structures which, in turn, prevents domain II from adopting the conformation required for dimerization. Since the receptor cannot adopt the conformation and location required for high-affinity ligand binding, it is also less likely that excess ligand could displace the bound antibody.

Implications for the mechanism of inhibition of EGFR by cetuximab

The structure presented here illustrates how cetuximab prevents ligand binding to EGFR, inhibits receptor dimerization, and thus blocks EGFR autophosphorylation and activation. This is believed to be the critical factor in the observed antitumor effects of this antibody in vivo (Mendelsohn and Baselga, 2003). The primary consequence of cetuximab binding to EGFR is to sterically block access of the growth factor to a key ligand binding region on domain III of the receptor. The ligand binding site on domain I is unaffected, but growth factor must engage sites on both domains I and III for high-affinity binding that activates the receptor, so efficient blockade of either one is sufficient to debilitate the receptor.

It is also clear from the structure that the EGFR extracellular region cannot adopt the extended dimerization-competent configuration depicted in Figures 1C and 1D while cetuximab remains bound. As mentioned above, steric clashes between the Fab and domain I will prevent this. Since ligand binding is normally required for the EGFR extracellular domain to adopt this extended configuration, and ligand binding is directly blocked by cetuximab, the importance of this conformational restriction for the inhibitory effects of the antibody is not immediately clear. However, the possibility remains that EGFR may under some circumstances be activated through mechanisms

that involve stabilization of the extended configuration without ligand binding, through homo- or heterodimerization with other activated ErbB receptor molecules (Sawano et al., 2002; Ververeer et al., 2000). Cetuximab binding will prevent this potential mode of activation, which may be relevant under conditions of receptor overexpression.

While direct inhibition of EGFR activation is considered the primary mechanism for the antitumor activity of cetuximab in vivo, additional mechanisms such as antibody-dependent cellular cytotoxicity (ADCC) and receptor internalization are also likely to play an important role. Indeed, the monovalent Fab fragment, which can elicit neither of these responses, is less effective than the bivalent mAb in inhibiting proliferation of cultured cells (Fan et al., 1993; Fan et al., 1994), although it is not without significant inhibitory effect. It is interesting to note that the intracellular fate of internalized cetuximab:EGFR complexes is likely to be different from that of growth factor:EGFR complexes. Whereas EGF binding is almost completely abolished at endosomal pH levels of ~5 (Ferguson et al., 2003), cetuximab binding to sEGFR is unchanged when the pH is reduced from pH 7 to pH 5 (data not shown). Thus, cetuximab is not likely to dissociate from the receptor in the low pH environment of the endosome, and the complex will be targeted for lysosomal degradation.

The structure of cetuximab in complex with sEGFR described here has implications for the design of small molecule agonists of EGFR. Attempts to block EGFR activation with antagonistic ligand analogs have not yet proven fruitful (Groenen et al., 1994; Matsunami et al., 1990). As described above, this may be due to the inherent flexibility of the ligand. A peptide with a more rigid scaffold that can mimic the high-affinity interaction of cetuximab with sEGFR may be more successful as an inhibitor than a simple ligand analog. Further, if such a molecule is fused to a bulky moiety that can sterically prevent the receptor from adopting the extended conformation, this could enhance the potency of the inhibitor. The definition of the epitope for cetuximab also serves as a focus to screen for somatic mutations in EGFR that may lead to an increased (or decreased) sensitivity to this EGFR-targeted drug. Somatic mutations in the kinase domain of EGFR have recently been correlated with the sensitivity of certain lung cancers to the EGFR-specific tyrosine kinase inhibitor (TKI) gefitinib (Lynch et al., 2004; Paez et al., 2004; Pao et al., 2004). Finally, it will be interesting to establish whether other anti-EGFR antibodies that are currently in clinical trials share a common epitope to that of cetuximab.

Experimental procedures

Protein expression and purification

sEGFR was produced and purified from baculovirus-infected Sf9 cells exactly as described (Ferguson et al., 2000), and was used without modification of its glycosylation state. This sEGFR was further purified by size exclusion chromatography (SEC) using a SEC250 column (BioRad) preequilibrated with 25 mM HEPES, 100 mM NaCl (pH 7.5). To produce isolated domain III of sEGFR (sEGFR-III), recombinant baculovirus was generated to direct expression of amino acids 310–514 of the mature EGFR extracellular region, plus a C-terminal hexahistidine tag, fused to the native signal peptide of EGFR. The sEGFR-III was expressed and purified exactly as for full-length sEGFR. The Fab fragment of cetuximab (FabC225) was prepared by treatment of the IgG protein with papain. The IgG protein (20 mg/ml) was incubated with papain (1:1000 w:w) at 37°C for one hour and the reaction stopped with iodoacetemide (75 mM final concentration). Undigested mAb and Fc fragments were removed by passing the mixture over a Protein-A column. The flowthrough from this column, containing FabC225, was used for crystallization of the Fab alone without further purification. To make FabC225:sEGFR complex, FabC225 was first purified on a SEC250 column exactly as for sEGFR. The FabC225 containing fractions were concentrated and mixed with sEGFR to give a 2-fold molar excess of Fab, and FabC225:sEGFR complex was separated from excess Fab using the same SEC column. Fractions containing the FabC225:sEGFR complex, as confirmed by SDS-PAGE, were concentrated to 11 mg/ml.

Crystallization and data collection

For crystallization of FabC225 alone, the flowthrough from the Protein-A column was buffer-exchanged into 100 mM NaCl, 10 mM Tris (pH 8.5), and adjusted to 22 mg/ml. Crystals were obtained by the vapor diffusion method. Equal volumes of FabC225 solution were mixed with a solution containing 1.8 M ammonium sulfate, 100 mM sodium citrate at pH 6.25, and equilibrated over a reservoir of this solution. Large single crystals were cryostabilized by rapid stepwise equilibration in solutions of reservoir containing increasing concentrations of glycerol (10%, 20%, and 30% volume/volume) and were flash frozen in liquid nitrogen. Data were collected at the National Synchrotron Light Source (NSLS) beamline X9A, using a MAR 165 CCD detector, and were processed using HKL (Otwinowski and Minor, 1997).

The purified FabC225:sEGFR complex was buffer-exchanged into 25 mM HEPES (pH 7.5), containing 50 mM NaCl, and was crystallized by the hanging drop vapor diffusion method from a drop containing equal parts of a 78 μM FabC225:sEGFR complex solution and reservoir solution of 15% PEG 3350, 250 mM $(NH_4)_2SO_4$, 100 mM Imidazole, 10 mM $CdCl_2$ (pH 7.5). Streak seeding was used to produce large (0.08 × 0.08 × 0.6 mm) single crystals. Crystals were cryostabilized with a brief exposure to 15% PEG 3350, 15% Ethylene Glycol, 250 mM $(NH_4)_2SO_4$, 100 mM Imidazole, 10 mM $CdCl_2$ (pH 7.5), and were flash frozen in liquid nitrogen. Data were collected at the Cornell High Energy Synchrotron Source (CHESS) beamline A1, using an ADSC Quantum-210 CCD detector, and were processed using HKL2000 (Otwinowski and Minor, 1997).

Structure determination and refinement

Coordinates of the FabC225 and the FabC225:sEGFR structures have been deposited with the RCSB protein data bank (PDB id codes 1YY8 and 1YY9, respectively). The structure of the FabC225 was solved by molecular replacement (MR) methods using the program AMORE (CCP4, 1994). Separate search models were selected for the variable (Fv) and constant (Fc) regions on the basis of sequence identity, the Fv region of the antibody 40-50 (PDB id 1IBG) (Jeffrey et al., 1995), and the Fc region from the human antibody Ctm01 (PDB id 1AD9) (Banfield et al., 1997). Both molecules in the asymmetric unit were located. The model was rebuilt using O (Jones et al., 1991) and refined using CNS (Brunger et al., 1998).

To solve the FabC225:sEGFR complex, search models for MR were derived from the coordinates of tethered sEGFR (PDB id 1NQL) and of the structure of FabC225 alone. An initial solution was found for a domain I/II fragment (amino acids 5–240) combined with a domain III fragment of sEGFR using the dyad option of MOLREP (CCP4, 1994) to search for the best relative orientation of these two fragments. With the solution for these fragments fixed, a solution for the Fab fragment was found. Rigid body refinement with CNS was used to optimize the orientation of the individual subdomains of FabC225. Following several rounds of model building using O (Jones et al., 1991) and refinement using CNS (Brunger et al., 1998), interpretable density for the remaining portions of sEGFR (C-terminal part of domain II and domain IV) could be seen in composite simulated-annealing omit-maps (calculated with CNS). The final stages of refinement employed TLS refinement (Winn et al., 2001) with anisotropic motion tensors refined for each of the four domains of sEGFR and each domain of FabC225, using REFMAC5 (CCP4, 1994).

Generation of binding site sEGFR mutations

Standard PCR-directed mutagenesis strategies were used to produce the appropriate DNA in the pFastBac vector. Targeted residues were mutated to the corresponding amino acid found at that position in *Drosophila* EGFR (DER), or to alanine if the position in DER was conserved (DER does not bind to human EGF or to cetuximab). The following mutations were made:

Q384A, Q408M/Q409E, Q384A/Q408M/Q409E, and D335T/F357A. The generation of baculovirus and overexpression and purification of the proteins in Sf9 cells were exactly as reported for wild-type sEGFR (Ferguson et al., 2000).

Binding studies

Surface plasmon resonance (SPR) binding experiments were performed on a BIAcore 3000 instrument at 25°C in buffer containing 10 mM HEPES buffer (pH 8.0), 150 mM NaCl, 3 mM EDTA, and 0.005% Tween 20 (HBS-EP8). EGF-agonists (200 μg/ml) were coupled to a CM5 BIAcore sensor chip using standard amine coupling. Optimal coupling was obtained in 10 mM sodium acetate at pH 4.0 for EGF and TGFα. Binding of sEGFR to these immobilized ligands was performed and analyzed exactly as described (Ferguson et al., 2000). FabC225 was coupled to a separate sensor chip using amine coupling. FabC225 was diluted to 50 μg/ml in 10 mM sodium acetate at pH 5.5 and passed over the activated surface for 5 min at a flow rate 10 μl/minute. The binding of sEGFR to this surface was determined exactly as for sEGFR binding to immobilized EGF with the following modifications: a longer contact time was used (10 μl/min for 25 min; 250 μl injection) to ensure that equilibrium was reached in binding of sEGFR to the surface even at low concentration, and the surface was regenerated between data points with two 5 μl injections of 10 mM glycine (pH 2.5), 1 M NaCl to rapidly remove residual bound sEGFR. This regeneration did not impair the binding of sEGFR to FabC225; the observed response for a control sEGFR sample is constant over multiple cycles of binding and regeneration. The effect of added FabC225 upon the binding of sEGFR to immobilized ligand was determined using the ligand chip described above. Binding was measured for a series of samples containing 600 nM sEGFR and increasing molar excesses of FabC225. Data were analyzed using Prism 4 (GraphPad Software, Inc.).

Supplemental data

Supplemental Figure S1 can be found at http://www.cancercell.org/cgi/content/full/7/4/301/DC1/.

Acknowledgments

We thank Mark Lemmon, Dan Leahy, and members of the Ferguson laboratory for valuable discussions and critical comments on the manuscript. The research of K.M.F. is supported by a Career Award in the Biomedical Sciences from the Burroughs Wellcome Fund and by a National Cancer Institute grant K01-CA092246. S.L was supported in part by NIH training grant T32-HL007027. This work is based upon research conducted at the Cornell High Energy Synchrotron Source (CHESS), which is supported by the National Science Foundation under award DMR 97-13424, using the Macromolecular Diffraction at CHESS (MacCHESS) facility, which is supported by award RR-01646 from the National Institutes of Health, through its National Center for Research Resources. P.K. is an employee of ImClone Systems Incorporated, the manufacturer of the drug Erbitux (cetuximab).

Received: January 15, 2005
Revised: February 25, 2005
Accepted: March 2, 2005
Published: April 18, 2005

References

Agus, D.B., Akita, R.W., Fox, W.D., Lewis, G.D., Higgins, B., Pisacane, P.I., Lofgren, J.A., Tindell, C., Evans, D.P., Maiese, K., et al. (2002). Targeting ligand-activated ErbB2 signaling inhibits breast and prostate tumor growth. Cancer Cell *2*, 127–137.

Arteaga, C.L. (2002). Overview of epidermal growth factor receptor biology and its role as a therapeutic target in human neoplasia. Semin. Oncol. *29*, 3–9.

Arteaga, C.L. (2003). ErbB-targeted therapeutic approaches in human cancer. Exp. Cell Res. *284*, 122–130.

Banfield, M.J., King, D.J., Mountain, A., and Brady, R.L. (1997). VL:VH domain rotations in engineered antibodies: Crystal structures of the Fab fragments from two murine antitumor antibodies and their engineered human constructs. Proteins *29*, 161–171.

Boerner, J.L., Danielsen, A., and Maihle, N.J. (2003). Ligand-independent oncogenic signaling by the epidermal growth factor receptor: v-ErbB as a paradigm. Exp. Cell Res. *284*, 111–121.

Brunger, A.T., Adams, P.D., Clore, G.M., DeLano, W.L., Gros, P., Grosse-Kunstleve, R.W., Jiang, J.S., Kuszewski, J., Nilges, M., Pannu, N.S., et al. (1998). Crystallography & NMR system: A new software suite for macromolecular structure determination. Acta Crystallogr. D Biol. Crystallogr. *54*, 905–921.

Burgess, A.W., Cho, H.S., Eigenbrot, C., Ferguson, K.M., Garrett, T.P., Leahy, D.J., Lemmon, M.A., Sliwkowski, M.X., Ward, C.W., and Yokoyama, S. (2003). An open-and-shut case? Recent insights into the activation of EGF/ErbB receptors. Mol. Cell *12*, 541–552.

CCP4 (Collaborative Computational Project, Number 4) (1994). The CCP4 suite: Programs for protein crystallography. Acta Crystallogr. D Biol. Crystallogr. *50*, 760–763.

Cho, H.S., and Leahy, D.J. (2002). Structure of the extracellular region of HER3 reveals an interdomain tether. Science *297*, 1330–1333.

Cho, H.S., Mason, K., Ramyar, K.X., Stanley, A.M., Gabelli, S.B., Denney, D.W., Jr., and Leahy, D.J. (2003). Structure of the extracellular region of HER2 alone and in complex with the Herceptin Fab. Nature *421*, 756–760.

Cooke, R.M., Wilkinson, A.J., Baron, M., Pastore, A., Tappin, M.J., Campbell, I.D., Gregory, H., and Sheard, B. (1987). The solution structure of human epidermal growth factor. Nature *327*, 339–341.

Fan, Z., Masui, H., Altas, I., and Mendelsohn, J. (1993). Blockade of epidermal growth factor receptor function by bivalent and monovalent fragments of 225 anti-epidermal growth factor receptor monoclonal antibodies. Cancer Res. *53*, 4322–4328.

Fan, Z., Lu, Y., Wu, X., and Mendelsohn, J. (1994). Antibody-induced epidermal growth factor receptor dimerization mediates inhibition of autocrine proliferation of A431 squamous carcinoma cells. J. Biol. Chem. *269*, 27595–27602.

Ferguson, K.M., Darling, P.J., Mohan, M.J., Macatee, T.L., and Lemmon, M.A. (2000). Extracellular domains drive homo- but not hetero-dimerization of erbB receptors. EMBO J. *19*, 4632–4643.

Ferguson, K.M., Berger, M.B., Mendrola, J.M., Cho, H.S., Leahy, D.J., and Lemmon, M.A. (2003). EGF activates its receptor by removing interactions that autoinhibit ectodomain dimerization. Mol. Cell *11*, 507–517.

Franklin, M.C., Carey, K.D., Vajdos, F.F., Leahy, D.J., de Vos, A.M., and Sliwkowski, M.X. (2004). Insights into ErbB signaling from the structure of the ErbB2-pertuzumab complex. Cancer Cell *5*, 317–328.

Garrett, T.P., McKern, N.M., Lou, M., Elleman, T.C., Adams, T.E., Lovrecz, G.O., Zhu, H.J., Walker, F., Frenkel, M.J., Hoyne, P.A., et al. (2002). Crystal structure of a truncated epidermal growth factor receptor extracellular domain bound to transforming growth factor alpha. Cell *110*, 763–773.

Gill, G.N., Kawamoto, T., Cochet, C., Le, A., Sato, J.D., Masui, H., McLeod, C., and Mendelsohn, J. (1984). Monoclonal anti-epidermal growth factor receptor antibodies which are inhibitors of epidermal growth factor binding and antagonists of epidermal growth factor binding and antagonists of epidermal growth factor-stimulated tyrosine protein kinase activity. J. Biol. Chem. *259*, 7755–7760.

Goldstein, N.I., Prewett, M., Zuklys, K., Rockwell, P., and Mendelsohn, J. (1995). Biological efficacy of a chimeric antibody to the epidermal growth factor receptor in a human tumor xenograft model. Clin. Cancer Res. *1*, 1311–1318.

Graham, J., Muhsin, M., and Kirkpatrick, P. (2004). Cetuximab. Nat. Rev. Drug Discov. *3*, 549–550.

Groenen, L.C., Nice, E.C., and Burgess, A.W. (1994). Structure-function relationships for the EGF/TGF-alpha family of mitogens. Growth Factors *11*, 235–257.

Gullick, W.J. (1991). Prevalence of aberrant expression of the epidermal growth factor receptor in human cancers. Br. Med. Bull. *47*, 87–98.

Holbro, T., and Hynes, N.E. (2004). ErbB receptors: Directing key signaling networks throughout life. Annu. Rev. Pharmacol. Toxicol. *44*, 195–217.

Honig, B., and Nicholls, A. (1995). Classical electrostatics in biology and chemistry. Science *268*, 1144–1149.

Jeffrey, P.D., Schildbach, J.F., Chang, C.Y., Kussie, P.H., Margolies, M.N., and Sheriff, S. (1995). Structure and specificity of the anti-digoxin antibody 40–50. J. Mol. Biol. *248*, 344–360.

Jones, T.A., Zou, J.Y., Cowan, S.W., and Kjeldgaard, M. (1991). Improved methods for building protein models in electron density maps and the location of errors in these models. Acta Crystallogr. A *47*, 110–119.

Kawamoto, T., Sato, J.D., Le, A., Polikoff, J., Sato, G.H., and Mendelsohn, J. (1983). Growth stimulation of A431 cells by epidermal growth factor: Identification of high-affinity receptors for epidermal growth factor by an anti-receptor monoclonal antibody. Proc. Natl. Acad. Sci. USA *80*, 1337–1341.

Klijn, J.G., Berns, P.M., Schmitz, P.I., and Foekens, J.A. (1992). The clinical significance of epidermal growth factor receptor (EGF-R) in human breast cancer: A review on 5232 patients. Endocr. Rev. *13*, 3–17.

Kline, T.P., Brown, F.K., Brown, S.C., Jeffs, P.W., Kopple, K.D., and Mueller, L. (1990). Solution structures of human transforming growth factor alpha derived from 1H NMR data. Biochemistry *29*, 7805–7813.

Kohda, D., Odaka, M., Lax, I., Kawasaki, H., Suzuki, K., Ullrich, A., Schlessinger, J., and Inagaki, F. (1993). A 40-kDa epidermal growth factor/transforming growth factor alpha-binding domain produced by limited proteolysis of the extracellular domain of the epidermal growth factor receptor. J. Biol. Chem. *268*, 1976–1981.

Lawrence, M.C., and Colman, P.M. (1993). Shape complementarity at protein/protein interfaces. J. Mol. Biol. *234*, 946–950.

Lemmon, M.A., Bu, Z., Ladbury, J.E., Zhou, M., Pinchasi, D., Lax, I., Engelman, D.M., and Schlessinger, J. (1997). Two EGF molecules contribute additively to stabilization of the EGFR dimer. EMBO J. *16*, 281–294.

Li, Y., Li, H., Yang, F., Smith-Gill, S.J., and Mariuzza, R.A. (2003). X-ray snapshots of the maturation of an antibody response to a protein antigen. Nat. Struct. Biol. *10*, 482–488.

Lo Conte, L., Chothia, C., and Janin, J. (1999). The atomic structure of protein-protein recognition sites. J. Mol. Biol. *285*, 2177–2198.

Lu, H.S., Chai, J.J., Li, M., Huang, B.R., He, C.H., and Bi, R.C. (2001). Crystal structure of human epidermal growth factor and its dimerization. J. Biol. Chem. *276*, 34913–34917.

Lynch, T.J., Bell, D.W., Sordella, R., Gurubhagavatula, S., Okimoto, R.A., Brannigan, B.W., Harris, P.L., Haserlat, S.M., Supko, J.G., Haluska, F.G., et al. (2004). Activating mutations in the epidermal growth factor receptor underlying responsiveness of non-small-cell lung cancer to gefitinib. N. Engl. J. Med. *350*, 2129–2139.

Masui, H., Kawamoto, T., Sato, J.D., Wolf, B., Sato, G., and Mendelsohn, J. (1984). Growth inhibition of human tumor cells in athymic mice by anti-epidermal growth factor receptor monoclonal antibodies. Cancer Res. *44*, 1002–1007.

Matsunami, R.K., Campion, S.R., Niyogi, S.K., and Stevens, A. (1990). Analogs of human epidermal growth factor which partially inhibit the growth factor-dependent protein-tyrosine kinase activity of the epidermal growth factor receptor. FEBS Lett. *264*, 105–108.

McDonald, I.K., and Thornton, J.M. (1994). Satisfying hydrogen bonding potential in proteins. J. Mol. Biol. *238*, 777–793.

Mendelsohn, J. (1988). Anti-EGF receptor monoclonal antibodies: Biological studies and potential clinical applications. Trans. Am. Clin. Climatol. Assoc. *100*, 31–38.

Mendelsohn, J. (2002). Targeting the epidermal growth factor receptor for cancer therapy. J. Clin. Oncol. *20*, 1S–13S.

Mendelsohn, J., and Baselga, J. (2003). Status of epidermal growth factor receptor antagonists in the biology and treatment of cancer. J. Clin. Oncol. *21*, 2787–2799.

Montelione, G.T., Wuthrich, K., Nice, E.C., Burgess, A.W., and Scheraga, H.A. (1987). Solution structure of murine epidermal growth factor: Determination of the polypeptide backbone chain-fold by nuclear magnetic resonance and distance geometry. Proc. Natl. Acad. Sci. USA *84*, 5226–5230.

Normanno, N., Bianco, C., De Luca, A., and Salomon, D. (2001). The role of EGF-related peptides in tumor growth. Front. Biosci. *6*, D685–D707.

Ogiso, H., Ishitani, R., Nureki, O., Fukai, S., Yamanaka, M., Kim, J.H., Saito, K., Sakamoto, A., Inoue, M., Shirouzu, M., et al. (2002). Crystal structure of the complex of human epidermal growth factor and receptor extracellular domains. Cell *110*, 775–787.

Otwinowski, Z., and Minor, W. (1997). Processing of X-ray diffraction data collected in oscillation mode. In Macromolecular Crystallography, Volume 276, C.W. Carter and R.M. Sweet, eds. (New York: Academic Press), pp. 307–326.

Paez, J.G., Janne, P.A., Lee, J.C., Tracy, S., Greulich, H., Gabriel, S., Herman, P., Kaye, F.J., Lindeman, N., Boggon, T.J., et al. (2004). EGFR mutations in lung cancer: Correlation with clinical response to gefitinib therapy. Science *304*, 1497–1500.

Pao, W., Miller, V., Zakowski, M., Doherty, J., Politi, K., Sarkaria, I., Singh, B., Heelan, R., Rusch, V., Fulton, L., et al. (2004). EGF receptor gene mutations are common in lung cancers from "never smokers" and are associated with sensitivity of tumors to gefitinib and erlotinib. Proc. Natl. Acad. Sci. USA *101*, 13306–13311.

Sainsbury, J.R., Malcolm, A.J., Appleton, D.R., Farndon, J.R., and Harris, A.L. (1985). Presence of epidermal growth factor receptor as an indicator of poor prognosis in patients with breast cancer. J. Clin. Pathol. *38*, 1225–1228.

Salomon, D.S., Brandt, R., Ciardiello, F., and Normanno, N. (1995). Epidermal growth factor-related peptides and their receptors in human malignancies. Crit. Rev. Oncol. Hematol. *19*, 183–232.

Sato, J.D., Kawamoto, T., Le, A.D., Mendelsohn, J., Polikoff, J., and Sato, G.H. (1983). Biological effects in vitro of monoclonal antibodies to human epidermal growth factor receptors. Mol. Biol. Med. *1*, 511–529.

Sawano, A., Takayama, S., Matsuda, M., and Miyawaki, A. (2002). Lateral propagation of EGF signaling after local stimulation is dependent on receptor density. Dev. Cell *3*, 245–257.

Sheinerman, F.B., Norel, R., and Honig, B. (2000). Electrostatic aspects of protein-protein interactions. Curr. Opin. Struct. Biol. *10*, 153–159.

Sheinerman, F.B., and Honig, B. (2002). On the role of electrostatic interactions in the design of protein-protein interfaces. J. Mol. Biol. *318*, 161–177.

Sundberg, E.J., and Mariuzza, R.A. (2002). Molecular recognition in antibody-antigen complexes. Adv. Protein Chem. *61*, 119–160.

Tappin, M.J., Cooke, R.M., Fitton, J.E., and Campbell, I.D. (1989). A high-resolution 1H-NMR study of human transforming growth factor alpha. Structure and pH-dependent conformational interconversion. Eur. J. Biochem. *179*, 629–637.

Verveer, P.J., Wouters, F.S., Reynolds, A.R., and Bastiaens, P.I. (2000). Quantitative imaging of lateral ErbB1 receptor signal propagation in the plasma membrane. Science *290*, 1567–1570.

Winn, M.D., Isupov, M.N., and Murshudov, G.N. (2001). Use of TLS parameters to model anisotropic displacements in macromolecular refinement. Acta Crystallogr. D Biol. Crystallogr. *57*, 122–133.

Accession numbers

Coordinates of the FabC225 and the FabC225:sEGFR structures have been deposited with the RCSB protein data bank (PDB id codes 1YY8 and 1YY9 respectively).